

Surface polaritons on gold-wire gratings

Hans Lochbihler

Max-Planck-Institut für Extraterrestrische Physik, 85748 Garching bei München, Germany

(Received 22 November 1993; revised manuscript received 4 March 1994)

A resonance phenomenon in the zeroth diffraction order of a gold-wire grating is explained by the excitation of surface polaritons. This effect is connected with a strong enhancement of the electromagnetic fields on the wire surface and consequently with a peak of power losses in the grating material. Measurements of the zeroth-order transmittance have been performed on gold gratings with periods of 1 and 2 micrometers in the near-infrared region which are in agreement with theoretical results. Furthermore, dispersion relations of the first-order coupling mode are presented having large energy gaps in the center of the Brillouin zone. It is shown that this energy gap strongly depends on the wire profile. In this coupling branch, however, practically no dispersion could be observed for optical wavelengths less than the grating period.

I. INTRODUCTION

Surface polaritons (SP's) may be excited on periodically corrugated metal-vacuum interfaces, when the momentum component of the impinging photons, which is parallel to the surface, differs from that of the SP by a nonzero number of reciprocal-lattice vectors G . The occurrence of SP's coincidences with the observation of resonance anomalies in the diffracted orders.¹ Numerous experiments have been performed on sinusoidal reflection gratings of rather small amplitudes compared with their periods²⁻⁴ such that the corrugation could be considered as a small perturbation of a flat metallic surface. The measured dispersion relations having gaps in energy and momentum, respectively, could be confirmed by means of theories based on the Rayleigh hypothesis⁵ and the extinction theorem.⁶ The excitation of SP's on lamellar (square-wave) gratings also with larger amplitudes has been theoretically studied in Refs. 7-9, numerically as well as experimentally in Refs. 10 and 11.

In this paper, an experimental and numerical study of SP excitation on metallic *wire gratings* is presented. The technique of measurement as well as the results substantially differ from the above-mentioned investigations. The dispersion of SP's is exemplified on gold gratings with a period $d = 2 \mu\text{m}$. The influence of the wire profile to the energy gap is investigated for a large number of gratings having a period $d = 0.9911 \mu\text{m}$.

II. EXPERIMENT

The wire gratings with periods $d = 2$ and $0.9911 \mu\text{m}$, respectively, have been manufactured from gold by a photochemical process.¹² The individual wires, which have an approximately rectangular cross section, are held on its position by a coarse support grid. This structure is illuminated by p -polarized light (\vec{E} perpendicular to the wires), where its free-space wave vector k_0 is perpendicular to the wires and forms an angle Θ_0 with the normal vector of the grating plane (Fig. 1). The photons couple to the SP's with a momentum transfer nG ($n = \pm 1, \pm 2,$

$\pm 3, \dots$) to the grating, where $G = 2\pi/d$ is the reciprocal-lattice vector and n is the coupling order. As shown in the k -space diagram of Fig. 1 for optical wavelengths $\lambda > d(1 + |\sin\Theta_0|)$, only the zeroth transmitted and reflected orders propagate and the first evanescent orders can excite SP's, when the relation $\pm k_{\text{SP}} = k_0 \sin\Theta_0 \mp G$ is fulfilled, where k_{SP} denotes the real part of the SP wave vector. As a result of energy dissipation due to this excitation, dips of intensity can be observed in the propagating orders.

In contrast to the widely investigated reflection gratings, this wire structure permits the measurement of zeroth-order *transmittance* as a function of wavelength and angle of incidence. The measurements have been performed by means of a Cary 5 spectrophotometer

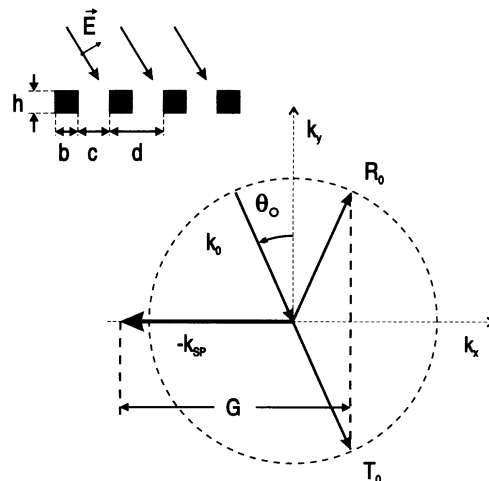


FIG. 1. The wire grating (period d , wire width b , width of free space $c = d - b$, and wire height h) is illuminated with p -polarized light by an angle of incidence Θ_0 . SP's of the -1 order coupling mode are excited when the relation $k_{\text{SP}} = G - k_0 \sin\Theta_0$ holds, where $G = 2\pi/d$ denotes the reciprocal-lattice vector. In this sketch only the zeroth diffraction orders (T_0, R_0) can propagate.

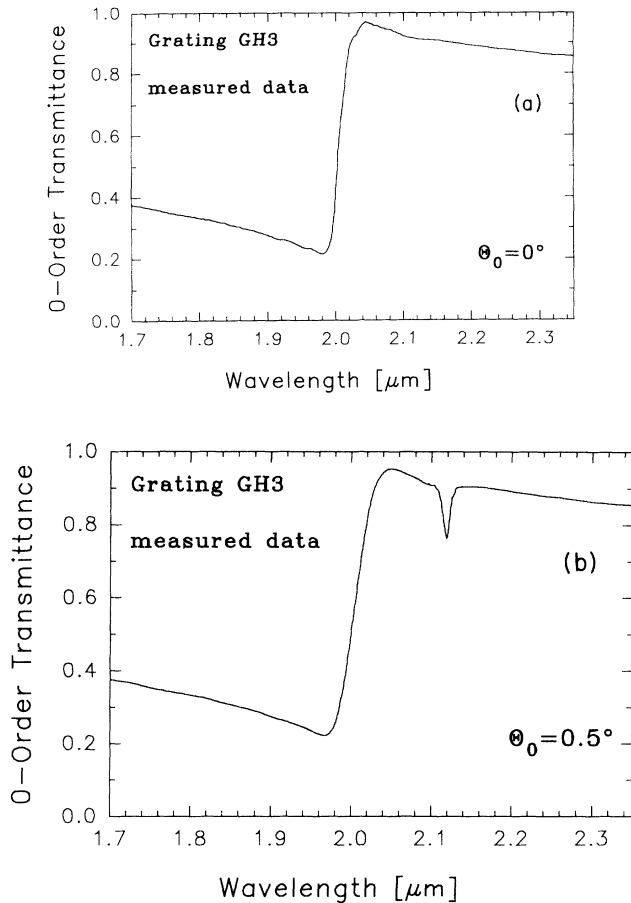


FIG. 2. Measured zeroth-order transmittance as a function of wavelength of the gold-wire grating *GH3* ($d=2\ \mu\text{m}$) for p -polarized light. The angle of incidence is (a) $\Theta_0=0^\circ$ and (b) $\Theta_0=0.5^\circ$.

(Varian Co.). For this purpose, the beam divergence of the spectrometer was reduced by aperture stops to 0.1° ; the gratings could be tilted within an angular accuracy of 0.03° . The spectral width of the monochromator was 1 nm. Figure 2 shows the measured transmittance of the grating *GH3* as a function wavelength (a) for normal incidence $\Theta_0=0^\circ$ and (b) for $\Theta_0=0.5^\circ$. The most obvious difference of both of these curves is the occurrence of a sharp resonant dip with its minimum transmittance on the wavelength $\lambda_r=2.118\ \mu\text{m}$ for the non-normal incidence $\Theta_0=0.5^\circ$.

III. THEORY

This diffraction behavior is now modeled by means of a modal formalism, which uses the surface impedance as boundary conditions on the wire surface. This approximative method, which was recently presented by Lochbihler and Depine,¹³ is particularly suited for highly conducting wire gratings with rectangular cross section. For highly conducting materials, such as gold in the infrared region, rigorous methods usually exhibit numerical difficulties or require rather complicated numerical treatments causing long computation times. In this case, the

electromagnetic field penetrates into the wires by the skin depth only and the wires are practically field-free in their interior. The problems encountered by the solution of Maxwell's equations inside the wires is bypassed if a surface-impedance boundary condition (SIBC) is imposed on the metallic boundaries.

The SIBC contains the following relation between the tangential components of the electric and magnetic fields at the boundary of a vacuum and a metal:

$$\mathbf{E}_\parallel = \mathbf{Z}\hat{\mathbf{n}} \times \mathbf{H}_\parallel, \quad (1)$$

where \mathbf{Z} is the surface impedance and $\hat{\mathbf{n}}$ denotes a normal unit vector on the boundary pointing into the free-space side. The approximation of a constant impedance $\mathbf{Z}=1/\nu$ (ν denotes the refractive index of the metal) yields good results compared with exact methods if the material is highly conducting.^{13,14}

For p polarization, we rewrite this boundary condition [Eq. (1)] by means of Maxwell's equations leading to

$$\frac{\partial f}{\partial \hat{\mathbf{n}}} = \frac{\mathbf{Z}k_0}{i} f = \eta f, \quad (2)$$

where $f(x,y)$ represents the spatial part of the component along the z axis of the magnetic field.

It is well known that the fields in the free half spaces above the top as well as below the bottom of the wires can be expressed in terms of plane-wave or Rayleigh expansions. The total field in the region $y > h/2$ contains the sum of the incident wave with its wave vector $k_0=\omega/c_0=2\pi/\lambda$ and the reflected waves, which gives

$$f(x,y) = \sum_{n=-\infty}^{\infty} \{R_n \exp[i\chi_n(y-h/2)] + \delta_{n,0} \exp[-i\chi_0(y-h/2)]\} \exp(i\alpha_n x). \quad (3)$$

The field below the grating region ($y \leq -h/2$) can be expressed by

$$f(x,y) = \sum_{n=-\infty}^{\infty} T_n \exp\{i[\alpha_n x - \chi_n(y+h/2)]\}, \quad (4)$$

where R_n , T_n are the complex amplitudes of the reflected and transmitted field, respectively. The coefficient

$$\alpha_n = k_0 \sin \Theta_0 + n \frac{2\pi}{d} \quad (5)$$

represents the tangential component of the k vector of a diffracted wave, where n is an integer. Its normal component is defined by

$$\chi_n = \begin{cases} \sqrt{k_0^2 - \alpha_n^2} & \text{if } |k_0| \geq |\alpha_n| \\ i\sqrt{\alpha_n^2 - k_0^2} & \text{if } |k_0| < |\alpha_n|, \end{cases} \quad (6)$$

which means that the wave is propagating if $|k_0| \geq |\alpha_n|$. The alternate case corresponds to evanescent waves traveling along the grating plane and exponentially damped in the normal direction.

In the modal method, the field within the grating region $|y| \leq h/2$ is expanded in a complete set of eigenfunctions, where each term obeys the wave equation and the appropriate boundary conditions. It is easy to prove that the functions

$$f(x, y) = \sum_{m=0}^{\infty} u_m(x) \left[a_m \frac{\sin(\mu_m y)}{\sin(\mu_m h/2)} + b_m \frac{\cos(\mu_m y)}{\cos(\mu_m h/2)} \right], \quad (7)$$

are eigenfunctions of the wave equation. Imposing the SIBC at $x=0, c$ we deduce the functions $u_m(x)$ for the air region between the wires,

$$u_m(x) = \frac{1}{\sqrt{I_m}} \left[\frac{\eta}{\beta_m} \sin \beta_m x + \cos \beta_m x \right], \quad (8)$$

with the normalization factor

$$I_m = \left[1 + \left(\frac{\eta}{\beta_m} \right)^2 \right] \frac{c}{2} + \frac{\eta}{\beta_m^2}. \quad (9)$$

The wave equation demands that the separation constants β_m and μ_m satisfy the relation $\beta_m^2 + \mu_m^2 = k_0^2$. The eigenvalues β_m have to be determined as the complex roots from the transcendental equation

$$\tan(\beta_m c) = \frac{2\eta\beta_m}{\beta_m^2 - \eta^2}. \quad (10)$$

By matching the Rayleigh and the modal field expansions at the boundaries $y=h/2$ and $y=-h/2$, and using the SIBC on the top and the bottom of the wires, respectively, we finally get a system of linear equations containing the unknown complex amplitudes R_n , T_n , a_m , and b_m . From this system, we easily evaluate the reflexion and transmission coefficients,

$$R_n = [Q_{p,n}^-]^{-1} [Q_{p,0}^+ + J_{p,m} (D_{1m} a_m + D_{2m} b_m)], \quad (11)$$

$$T_n = -[Q_{p,n}^-]^{-1} J_{p,m} (D_{1m} a_m - D_{2m} b_m), \quad (12)$$

with the mode amplitudes

$$a_m = (\delta_{j,m} - K_{j,n} [Q_{p,n}^-]^{-1} J_{p,m} D_{1m})^{-1} \times \frac{1}{2} K_{j,p} ([Q_{q,p}^-]^{-1} Q_{q,0}^+ + \delta_{p,0}) \quad (13)$$

and

$$b_m = (\delta_{j,m} - K_{j,n} [Q_{p,n}^-]^{-1} J_{p,m} D_{2m})^{-1} \times \frac{1}{2} K_{j,p} ([Q_{q,p}^-]^{-1} Q_{q,0}^+ + \delta_{p,0}), \quad (14)$$

and

$$D_{1m} = \mu_m \cot(\mu_m h/2), \quad (15)$$

$$D_{2m} = -\mu_m \tan(\mu_m h/2). \quad (16)$$

The matrix elements

$$J_{q,m} = \frac{1}{d} \int_0^c \exp(-i\alpha_q x) u_m(x) dx, \quad (17)$$

$$K_{j,n} = \int_0^c \exp(i\alpha_n x) u_j(x) dx, \quad (18)$$

and

$$Q_{q,p}^{\pm} = i\chi_q \delta_{q,p} \pm \frac{\eta}{d} \int_c^d \exp[i(\alpha_p - \alpha_q)x] dx \quad (19)$$

can be calculated analytically.

The roots β_m of Eq. (10) have to be determined numerically, which can be easily performed by a Newton-Raphson algorithm. In the exact modal method of Botten *et al.*,¹⁵ however, more sophisticated algorithms¹⁶ are needed for the solution of the corresponding eigenvalue equation. This is the reason that the computation time of the diffraction problem by means of the method presented here is approximately five times shorter compared with that exact method. But the more essential point is that the exact method exhibits numerical instabilities for highly conducting gratings, which are completely absent for the SIBC method. The main reason is that a part of the complex zeros having rather large imaginary parts converge very slowly against the real axis with increasing number m . Hence, it is quite difficult to construct an "as much complete as possible" set of eigenfunctions [Eq. (7)]. In the SIBC method, however, the complex roots of Eq. (10) converge rapidly against the real axis (see Fig. 3 in Ref. 13) and for the numerical calculation the criterion of completeness may be better satisfied as in that exact method.

It should be noted that the exact modal approach developed by Sheng, Stepleman, and Sanda¹⁰ for calculations of surface-plasmon excitations on square-wave gratings and its generalization by Lee and George⁸ to multilayer gratings is closely related to that formalism of Botten *et al.*

Furthermore, we obtain a "more physical" expression for the power losses in the wires compared with that in the exact method. Starting from the second Green's identity, the power losses normalized to the incident power P_{abs} can be derived as

$$P_{\text{abs}} = \frac{1}{2ik_0 d \cos \Theta_0} \oint_S \left[f \frac{\partial f^*}{\partial \hat{n}} - f^* \frac{\partial f}{\partial \hat{n}} \right] ds, \quad (20)$$

where the integral has to be determined along the wire surface. Finally, the expression for the power losses in the grating simplifies to

$$P_{\text{abs}} = \frac{\text{Re}Z}{d \cos \Theta_0} \oint_S |f|^2 ds, \quad (21)$$

if we impose the SIBC in Eq. (20).

For highly conducting materials, this expression contains a simple relation between the power losses and the electromagnetic fields on the surface, which means that $dP_{\text{abs}}/ds \propto |H_z|^2$ on the wire surface for p polarization.

IV. RESULTS

Figure 3 shows the calculated transmittance and the power losses P_{abs} for a gold-wire grating, which corresponds to the measurement in Fig. 2, assuming a rectangular cross section. The parameters width $b=0.653$

μm and height $h=0.556 \mu\text{m}$ of the profile have been reconstructed for the grating *GH3* by fitting an electromagnetic model to transmittance measurements.¹⁴ The complex refractive index of gold, which is used for numerical calculations, corresponds exactly to the same grating material as in the experiment (see Ref. 13).

In addition, these curves are compared with the numerical results obtained from the exact method after Boten *et al.* (crosses). The excellent coincidence of the rigorous formalism with the SIBC method—particularly in the resonance dip—confirms the validity of this approximative model for this spectral region.

These numerical considerations yield similar results for the transmittance as in the experiment, shown in Fig. 2. For non-normal incidence $\Theta_0=0.5^\circ$, a sharp resonance occurs in the transmittance and coincidentally in the power losses ($\lambda_r=2.113 \mu\text{m}$). Tilting the grating from normal incidence only by a half degree, the power losses arise

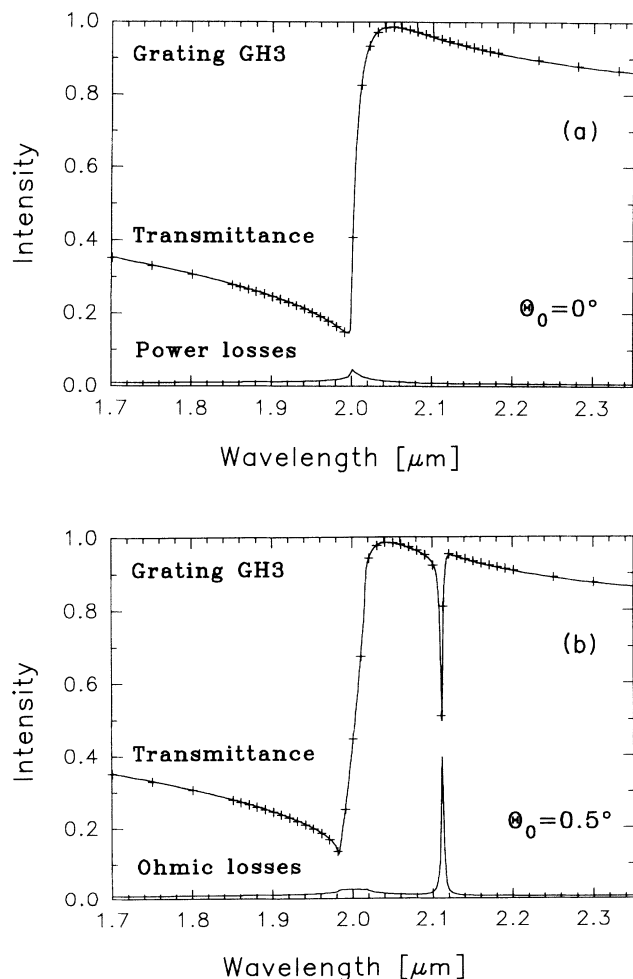


FIG. 3. Calculated transmittance and power losses for a gold-wire grating similar to that in Fig. 2: (a) $\Theta_0=0^\circ$ and (b) $\Theta_0=0.5^\circ$. In the theoretical model a rectangular wire geometry ($d=2 \mu\text{m}$, $b=0.653 \mu\text{m}$, $h=0.556 \mu\text{m}$) is assumed. The solid lines correspond to the results of the SIBC method, which are confirmed by the transmittance data obtained from the exact modal method (crosses).

from 0.9% up to 40% in this resonance. From Eq. (21), we deduce that the squared magnetic field on the wire surface is strongly enhanced compared with the field for normal incidence: on top of the wires by a factor of 16, on the bottom by a factor of 10, and on the walls by a factor of 125.

The other singularity in the transmittance curve could be identified as the Rayleigh anomaly, which results from the redistribution of energy when a propagating diffraction order becomes evanescent. In this case the power losses and, subsequently, the electromagnetic fields on the grating surface are enhanced.

The remaining discrepancies between theory and experiment are probably due to the simple approximation of the wire profile by a rectangle as well as the finite beam divergence and the limited monochromism of the spectrophotometer.

A microscopic analysis of the electromagnetic fields in the vicinity of the wires, which will be published elsewhere, shows that the individual wires act like electric dipole resonators with poles on the upper and lower wire surface. For the resonance in Fig. 3(b), the squared electric field on these sites is enhanced by more than a factor of 100 compared with that of the incident field. Although the wire grating represents a periodical arrangement of *isolated* objects, a concentrated energy stream propagates along the grating plane such as marked in Fig. 1 with the arrow $-k_{\text{SP}}$.

A. Dispersion of SP

Furthermore, the position of this resonance dip has been measured as a function of wavelength and angle of incidence Θ_0 . Following the suggestion of Weber and Mills,¹⁷ the transmittance minima around the $(-1, +1)$ minigap region have been determined from wavelength scans with *fixed* angle of incidence Θ_0 . The dispersion curves evaluated from these transmittance measurements on the grating *GH3* are presented in Fig. 4. The Rayleigh threshold, where the first diffracted order becomes evanescent, is marked by the dashed lines.

In the same manner as in the experiment, the dispersion relations have been numerically constructed by locating the transmittance dips in the (λ, Θ_0) plane (shown in Fig. 4 as solid lines), which confirm the experimental results. The lower curve exhibits an energy gap (energy difference between Rayleigh threshold and SP excitation) of 33 meV in the center of the Brillouin zone. It should be noted that the maximum of SP excitation occurs close to normal incidence ($\Theta_0=0.8^\circ$), where the power losses P_{abs} are approximately 50%. The higher-frequency branch coincident with the dip in the Rayleigh anomaly, however, is obviously nondispersive.

Figure 5 demonstrates the strong influence of the wire profile to the dispersion of SP's. The lower-frequency branch was experimentally obtained for three gold gratings ($d=2 \mu\text{m}$) with different wire profiles. The largest energy gap of 60 meV could be observed for the grating *GH1*. Now the influence of the wire width to this dispersion relation around the $(-1, +1)$ minigap region is numerically analyzed. Figure 6 shows the lower-frequency

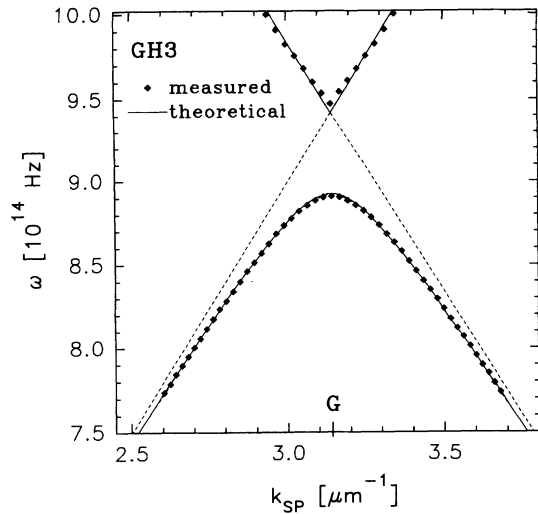


FIG. 4. Comparison of measured and calculated dispersion of the SP's (-1 and $+1$ order coupling mode) in the vicinity of the center of the Brillouin zone. The branch for $\lambda > d$ exhibits a large energy gap, while no dispersion occurs in the higher-frequency branch. The dashed lines indicate the Rayleigh threshold, where the first diffracted order becomes evanescent.

branches for gold-wire gratings of rectangular cross section with different wire width b and constant period $d = 2.0 \mu\text{m}$ and height $h = 0.8 \mu\text{m}$. Apparently, the quantity of the energy gap strongly depends on the width of the free space between the wires. For increasing width of the free space (1.0, 1.2, 1.4, 1.6 μm), the energy gap arises from 3, 31, 64 up to 88 meV. In all cases, no dispersion in the first-order coupling mode could be found for wavelengths $\lambda < d$. Since for these wavelengths the first diffracted orders are no longer evanescent, the coupling to SP's with a momentum transfer G to the grating becomes rather unlikely.

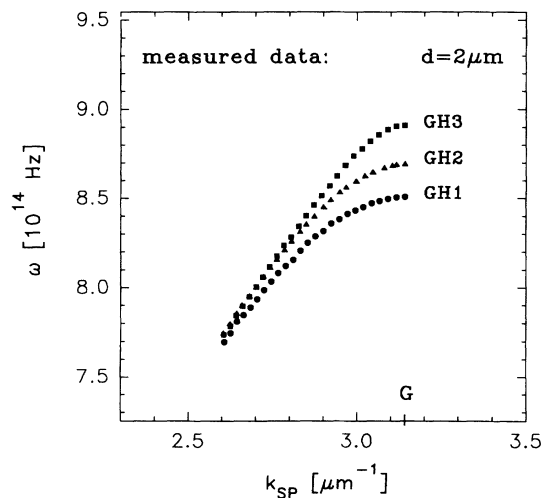


FIG. 5. Measured dispersion of the SP in the first coupling mode for gold gratings ($d = 2 \mu\text{m}$) with different wire profile. Grating GH1: $b = 0.62 \mu\text{m}$, $h = 0.96 \mu\text{m}$. Grating GH2: $b = 0.76 \mu\text{m}$, $h = 0.86 \mu\text{m}$. Grating GH3: $b = 0.65 \mu\text{m}$, $h = 0.56 \mu\text{m}$.

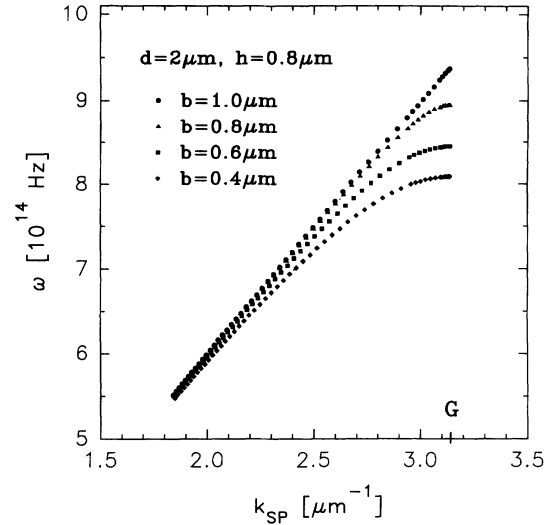


FIG. 6. Numerically obtained dispersion relations of the SP (first-order coupling mode) for a gold-wire grating with a rectangular cross section for different wire widths b in the vicinity of the center of the Brillouin zone. The period d and the wire height h are constant for all curves.

This behavior of the SP in the minigap region is quite different from those obtained by other authors^{3,4} for shallow sinusoidal gratings. Heitmann *et al.*,⁴ however, observed a strong asymmetry in the SP response, which has been interpreted with the interference of SP's propagating in opposite directions with different coupling mechanism.

Andrewartha, Fox, and Wilson⁷ theoretically studied the resonance anomalies on *lamellar gratings* by determining the poles of the mode amplitudes for complex wavelengths. The trajectories of these poles (real part) behave similar to the dispersion of SP's on wire gratings reported here. Moreover, in the case of infinite conductivity, these resonances are still present for both kinds of gratings, only the dip position is shifted compared with finite conducting materials.

B. Relation between energy gap and wire profile

The most characteristic feature of these dispersion curves is the energy gap, which we denote here as the energy difference between the Rayleigh threshold and the SP excitation for $\Theta_0 \rightarrow 0^\circ$. This parameter has been analyzed for a large number of gold gratings with a period $d = 0.9911 \mu\text{m}$. In the experiment, the transmittance dip has been located for an angle of incidence $\Theta_0 = 0.3^\circ$. For smaller angles the resonance dip practically does not change its position, but it becomes weaker and, therefore, harder to detect.

Figure 7(a) shows the energy gaps for gratings which have different wire width and approximately the same wire height ($h/d \approx 0.42$). These data are compared with theoretical values of the energy gap as a function of wire width. In Fig. 7(b), the relation between the energy gap and the wire height is demonstrated for gratings that have a constant wire width ($b/d \approx 0.48$). From these

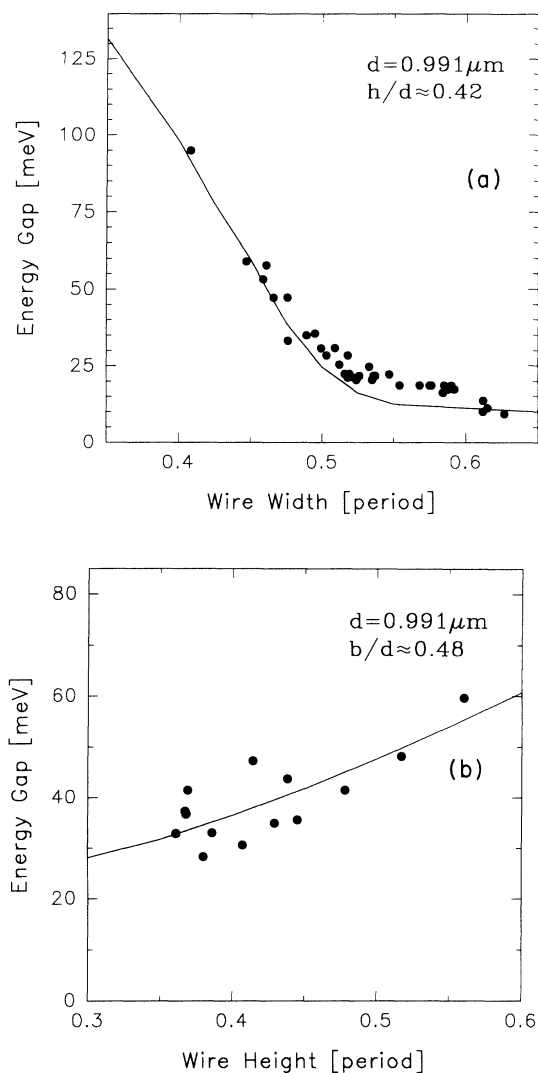


FIG. 7. Measured energy gaps of gratings which profiles have (a) different wire width and constant wire height and (b) different wire height and constant wire width. The solid line represents the theoretical data of the energy gap (a) as a function of wire width and fixed height $h/d=0.42$, and (b) as a function of wire height and fixed width $b/d=0.48$.

curves it is obvious that the quantity of energy gap depends much stronger on the wire width than on wire height if $b/d < 0.5$. Gratings with broader wires $b/d > 0.5$ do not seem to support a strong coupling

mechanism to SP excitation and the dispersion of SP's obviously becomes weak.

The deviations between the theoretical and experimental data are mainly due to the assumption that all gratings correspond to that constant wire parameter. Therefore, in Fig. 7(b), the discrepancy is larger than in Fig. 7(a), since an uncertainty in the wire width results in a greater variance of the energy gap around the predicted value than an uncertainty in the wire height would cause. Moreover, the real grating profile deviates somewhat from the rectangular shape which is assumed in the theory.

V. CONCLUSIONS

We have investigated a resonance phenomenon that occurs in the electromagnetic transmittance on gold-wire gratings. An approximated theory, which appears superior against existing rigorous formalisms for this application, was used to study the diffraction on highly conducting wire gratings. For reasons mentioned in the previous section, this resonance phenomenon on wire gratings is attributed to excitation of SP's, which hitherto was observed on sinusoidal and lamellar gratings. The dispersion of SP's has been studied in the first-order coupling mode for gratings with different wire profiles. In this coupling branch, however, practically no dispersion could be observed for optical wavelengths less than the grating period. This is due to the fact that for those wavelengths, the first diffracted orders are no longer evanescent.

Furthermore, it was demonstrated by measurements as well as by numerical calculations that the energy gap strongly depends on the wire profile. Subsequently, the knowledge of the dip position in the transmittance for near-normal incidence yields important information about the wire profile, which may be helpful for the characterization of those gratings. Due to the possibility of strong field enhancement on the wire surface, it is hoped that this kind of gratings could be used as an alternative tool for surface-enhanced Raman scattering.⁹

ACKNOWLEDGMENTS

I thank Ricardo A. Depine for fruitful discussions. This work was supported by BMFT Contract No. 01-00-90038.

¹See, for an overview, *Surface Polaritons*, edited by V. M. Agranovich and D. L. Mills (North-Holland, Amsterdam, 1982); H. R  ther, *Surface Plasmons on Smooth and Rough Surfaces and on Gratings* (Springer-Verlag, Berlin, 1988).

²R. H. Ritchie, E. T. Arakawa, J. J. Cowan, and R. N. Hamm, *Phys. Rev. Lett.* **21**, 1530 (1968).

³Y. J. Chen, E. S. Koteles, R. J. Seymour, G. J. Sonek, and J. M. Ballantyne, *Solid State Commun.* **46**, 95 (1983).

⁴D. Heitmann, N. Kroo, C. Schulz, and Zs. Szentirmay, *Phys.*

Rev. B **35**, 2660 (1987).

⁵N. E. Glass, M. Weber, and D. L. Mills, *Phys. Rev. B* **29**, 6548 (1984).

⁶M. Weber and D. L. Mills, *Phys. Rev. B* **27**, 2698 (1983).

⁷J. R. Andrewartha, J. R. Fox, and I. J. Wilson, *Opt. Acta* **26**, 69 (1979); **26**, 197 (1979).

⁸K. Lee and T. F. George, *Phys. Rev. B* **31**, 5106 (1985).

⁹A. Wirgin and A. A. Maradudin, *Prog. Surf. Sci.* **22**, 1 (1986).

¹⁰P. Sheng, R. S. Stepleman, and P. N. Sanda, *Phys. Rev. B* **26**,

- 2907 (1982).
- ¹¹S. H. Zaidi, M. Yousaf, and S. R. Brueck, *J. Opt. Soc. Am. B* **8**, 770 (1991); **8**, 1348 (1991).
- ¹²H. Bräuninger, H. Kraus, H. Dangschat, P. Predehl, and J. Trümper, *Appl. Opt.* **18**, 3502 (1979).
- ¹³H. Lochbihler and R. A. Depine, *Appl. Opt.* **32**, 3459 (1993).
- ¹⁴H. Lochbihler and R. A. Depine, *Opt. Commun.* **100**, 231 (1993); *J. Mod. Opt.* **40**, 1273 (1993).
- ¹⁵L. C. Botten, M. S. Craig, R. C. McPhedran, J. L. Adams, and J. R. Andrewartha, *Opt. Acta* **28**, 1087 (1981); **28**, 1103 (1981).
- ¹⁶L. C. Botten, M. S. Craig, and R. C. McPhedran, *Comput. Phys. Commun.* **29**, 245 (1983); G. Tayeb and R. Petit, *Opt. Acta* **31**, 1361 (1984).
- ¹⁷M. G. Weber and D. L. Mills, *Phys. Rev. B* **34**, 2893 (1986).

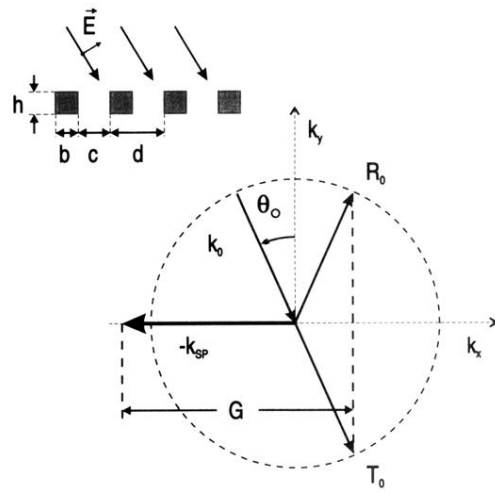


FIG. 1. The wire grating (period d , wire width b , width of free space $c=d-b$, and wire height h) is illuminated with p -polarized light by an angle of incidence Θ_0 . SP's of the -1 order coupling mode are excited when the relation $k_{sp}=G-k_0\sin\Theta_0$ holds, where $G=2\pi/d$ denotes the reciprocal-lattice vector. In this sketch only the zeroth diffraction orders (T_0, R_0) can propagate.